Space-based observations on annular solar eclipse of June 2020

On 21 June 2020, an annular solar eclipse phenomenon took place. The path of the 'ring of fire' spanned across Africa and Asia (Figure 1 *a*). In addition to the traditional methods of observing the solar eclipse through telescopes using solar filters or using solar projectors, this phenomenon can also be captured using satellite data. The shadow cast by the moon on the surface of the Earth leads to a drop in the solar flux over the Earth's surface, which can be recorded by space-based sensors in the visible – near-infrared spectral range. We have presented the natural colour composite images during eclipse conditions from three different satellite sensors, i.e. MOderate resolution Imaging Spectroradiometer (MODIS) over Terra/Aqua (https://modis.gsfc.nasa.gov/) and Visible Infrared Imaging Radiometer Suite (VIIRS) over NOAA-20 (https://data.nodc.noaa.gov/) (Figure 1 *b*). In these images, some of the regions appear much darker than the surroundings because of the reduction in the incident solar flux, leading to a decrease in the reflected energy. Hence, the darker shades indicate the moon's shadow on the Earth's surface, whereas white colour corresponds to the clouds. In Figure 1 *b*(i), the darkest portion of the shadow region is concentrated over Indo-Pakistan, and then it gradually, appears to shift with time towards the east (Figure 1 *b*(ii) and (iii)). However, each of these images is taken from polar/near-polar satellites that could enable only one snapshot for the eclipse. Hence, it is difficult to monitor the continuous track of the moon's shadow with time, from such platforms.

On the other hand, one can easily trace the path of the moon through the shift in its shadow over the Earth using data from geostationary satellites. In this context, we have used satellite images capturing the moon's shadow across different time stamps between 0600 and 0715 h UTC from the visible channel (500–720 nm) of Indian Space Research Organisation's (ISRO's) space-based Imager on the geostationary platforms (Indian National Satellite) INSAT-3D and INSAT-3DR[1,2]. These two satellites are positioned at different longitudes, i.e. 82°E (INSAT-3D) and 74°E (INSAT-3DR). Both the satellites capture the

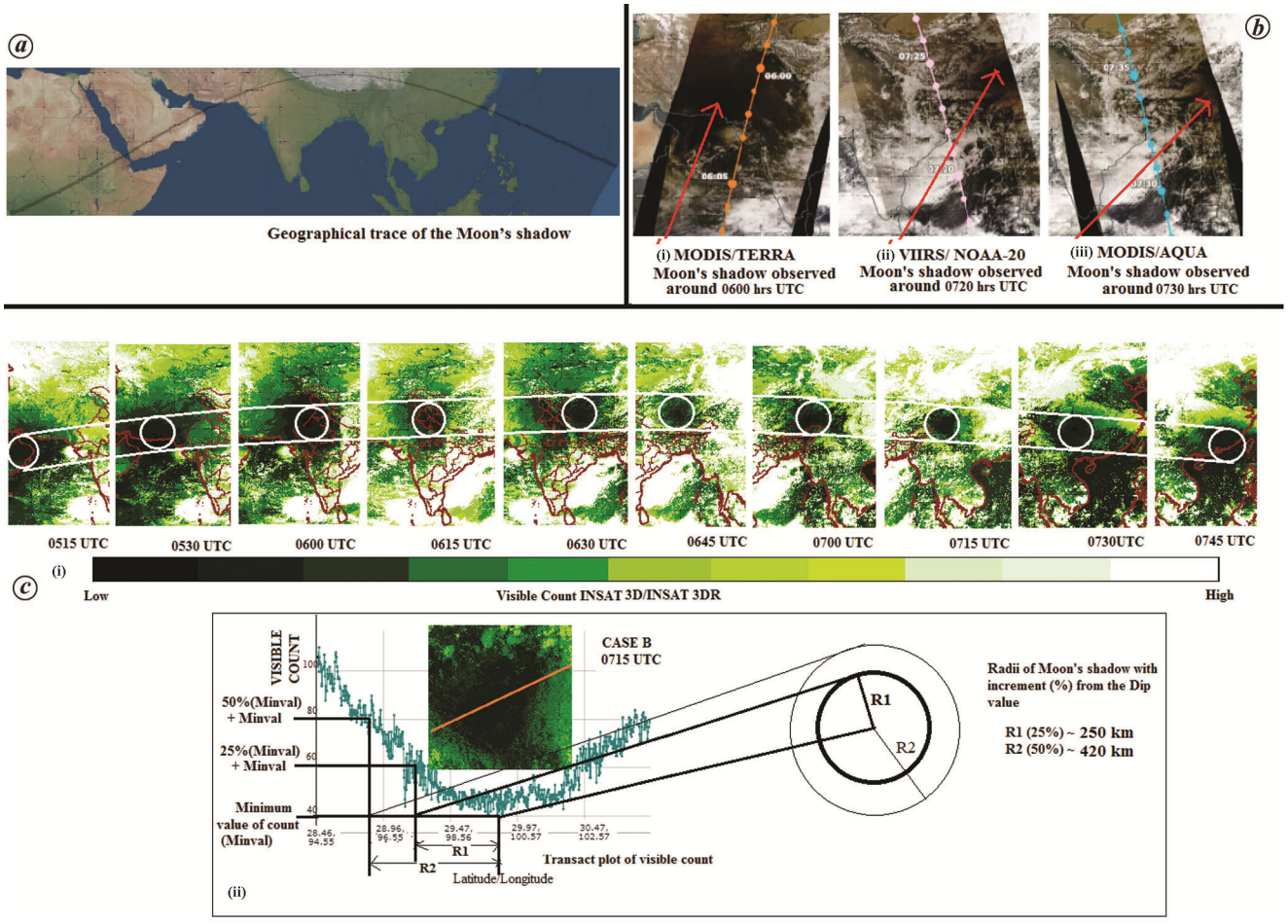

Figure 1. ***a***, Geographical trace of the moon's shadow (adapted from https://www.solar-eclipse.info/eclipse/images/worldmap_topo_2020-06-21.jpg/). ***b***, Moon's shadow over the Earth's surface from (i) MODIS/TERRA, (ii) VIIRS/NOAA-20 and (iii) MODIS/AQUA (source: https://worldview.Earthdata.nasa.gov/). ***c***, (i) Moon's shadow over the Earth as seen through INSAT-3D(3DR) at different time stamps (data download link: https://www.mosdac.gov.in/). (ii) Transect plot for one time frame (0715 h; time in UTC).

Earth's images at an interval of every 30 min. Hence, combining the images from both the sensors enabled us to have consecutive time frames after every 15 min (Figure 1 *c*(i)) (except for one time frame that was not available) during the eclipse conditions. For illustrative purpose, a pseudo-colour is assigned to these datasets, where darker shades correspond to the moon's shadow region, whereas the white colour indicates the clouds. Using these satellite images we could identify the centre of the dip in the signal and estimate the shadow region covered over the Earth's surface. As an illustration, we have provided the transect plot of the shadow region for one of the time frames (0715 h, UTC) (Figure 1 *c*(ii)). With respect to the centre of the dip, we estimated the radii of the moon's circular shadow where the visible count values changed by 25% and 50%. It should also be noted that these radii might not correspond to the size of the standard umbral/antumbral/penumbral shadows, but are an approximate estimation in terms of change in the intensity of solar flux with respect to the dip value for a particular transect under consideration. Nevertheless, the size of the shadow can be further refined by considering several transects in different directions and then comparing the estimated size for different time frames. As we have used the visible wavelength region, the presence of differential cloud cover at different locations might affect the estimation of the size of moon's shadow.

Furthermore, the impact of the solar eclipse can be observed in terms of a drop in the solar radiation (SR) and air temperature (AT) using data from automatic weather stations (AWS). We present here data from one such station of the Indian Institute of Remote Sensing (IIRS), ISRO, located at the agricultural research station of Nauni University, Bhota, Hamirpur, Himachal Pradesh. Figure 2 *a* shows a plot of shortwave SR (0.3–3.0 µm) and AT recorded on 21 June 2020. We can observe that SR had reduced by more than 95% (from 658 W/m^2 at 10:06 am to 21 W/m^2 at 11.46 am) during the peak of the solar eclipse and AT had reduced by ~2° (from 28.6°C at 10:01 am to 26.95°C at 12.06 pm). It is evident from the measurements that the reduction in AT was observed a little later than the instant at which minimum SR was recorded. This time lag can be understood in terms of the exchange of radiant energy between the Earth and the atmosphere[3]. The incident shortwave solar flux leads to warming of the Earth's surface. Following this, the warmed Earth's surface emits outgoing longwave radiation (OLR). This OLR is absorbed by the atmospheric gases which leads to a rise in the AT. Any change in the incoming solar radiation, thereby lead to a change in OLR, is not instantaneous; rather, it takes some time. This time lag can be observed during the entire duration of measurements between the variability of SR and AT. Further, for a quantitative assessment, one can compare the geophysical/atmospheric parameters (e.g. longwave radiation, temperature, etc.) from the Imager/Sounder products (INSAT-3D(3DR)) with respect to data from more weather stations equipped with full radiation sensors.

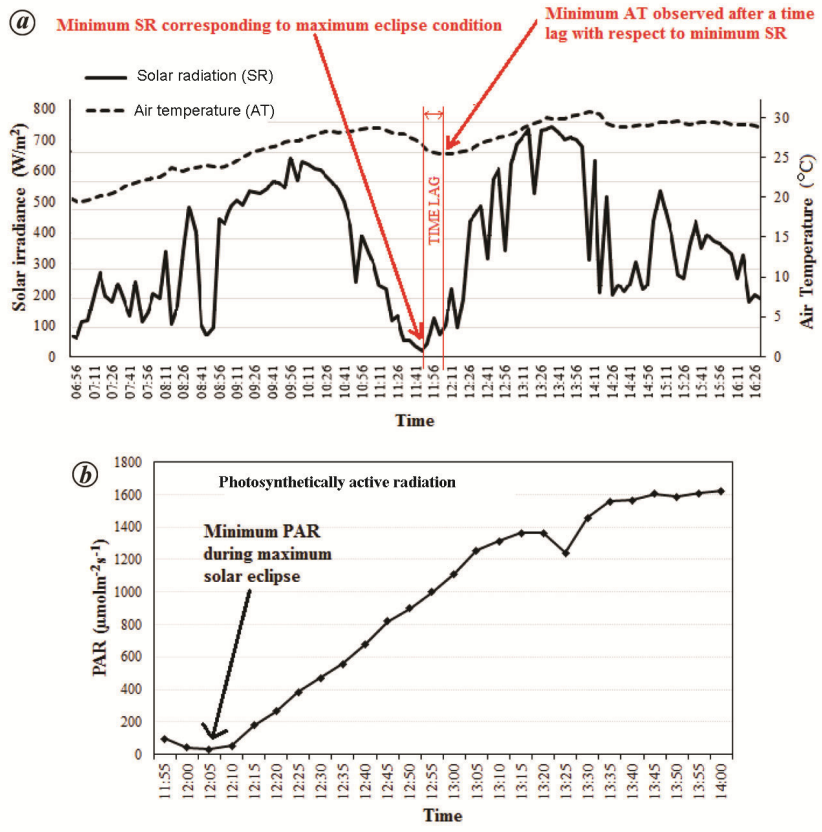

Figure 2. *In situ* measurements of (***a***) Solar radiation and air temperature over Bhota, Hamirpur. (***b***) Photosynthetically active radiation recorded at Indian Institute of Remote Sensing, Dehradun (source: IIRS/ISRO).

In addition, the effect of the eclipse could be observed as a manifestation of reduction in the photosynthetically active radiation (PAR) (400–700 nm) using *in situ* measurements. To this end, PAR measurements were carried out at 5-min interval using hand-held instruments (ACCUPAR LP-80, make: METER Group, Inc., USA) at IIRS, Dehradun (30.34°N, 78.04°E) beginning just before the maximum solar eclipse condition till the end of the phenomenon. We observed that at 11.55 am, the available PAR was 97 µmol m^{-2} s^{-1} (Figure 2 *b*). However, a further decline in PAR value was observed with a minimum value of 32 µmol m^{-2} s^{-1} at 12.05 pm. The PAR value observed during the eclipse was significantly low compared to the summer season daily average value of 426.63 µmol m^{-2} s^{-1} for Dehradun region[4]. Post 12:05 pm, the available PAR kept increasing (except at 1.25 pm, where we observed a drop in the value due to cloud cover) and became stable by 1.35 pm.

Such observations could be important from both scientific and application perspectives. For instance, a recent report has assessed the likely impacts of this annular solar eclipse on the solar power generation across different parts of India, wherein the solar generation reduction at the time of maximum solar eclipse with respect to a normal day was

estimated to be ~12 GW (ref. 5). Researchers interested in the mapping and assessment of the impacts of solar eclipse can utilize the remote-sensing datasets together with *in situ* measurements to have a better insight of such rare spectacular events.

1. https://mosdac.gov.in/data/doc/INSAT_3D_ATBD_MAY_2015.pdf (accessed on 22 June 2020).
2. Katti, V. R., Pratap, V. R., Dave, R. K. and Mankad, K. N., In SPIE Proceedings, GEOSS and Next-Generation Sensors and Missions, November 2006, 640709; https://doi.org/10.1117/12.697880.
3. Bristow, K. L. and Campbell, G. S., *Agric. For. Meteorol*., 1984, **31**, 159–166; https://doi.org/10.1016/0168-1923(84)90017-0.
4. Watham, T. *et al.*, *Biogeochemistry*, 2020, **151**, 291–311; https://doi.org/10.1007/s10533-020-00727-x.
5. https://posoco.in/wp-content/uploads/2020/06/Solar-Eclipse-dated-210620_likely-impacts-and-preparedness-A-report.pdf (accessed on 26 June 2020).

ACKNOWLEDGEMENTS. We thank the teams of MOSDAC/ISRO, WORLDVIEW/EARTHDATA and AWS/IIRS for providing access to the datasets.

Received 3 July 2020; revised accepted 22 December 2020

MANU MEHTA*
PRAKASH CHAUHAN
PRAVEEN THAKUR
TAIBANGANBA WATHAM
RITIKA SRINET

Indian Institute of Remote Sensing, ISRO,
4-Kalidas Road,
Dehradun 248 001, India
**For correspondence.*
e-mail: manu@iirs.gov.in

Natural occurrence of entomopathogens on the invasive fall armyworm, *Spodoptera frugiperda* (J.E. Smith) in South India

Biological invasions are quite frequent in recent years due to free trade and global warming. Fall armyworm (FAW), *Spodoptera frugiperda* which is a highly migratory polyphagous insect pest, has posed itself as a recent dreadful insect that invaded India in May 2018 on maize in Shivamogga and Davanagere districts of Karnataka, India[1]. FAW is one of the major production constraints of maize crop across the globe. *Spodoptera frugiperda* was reported to cause 62.5% plant damage on maize in Hassan district of Karnataka[2]. The management of *S. frugiperda* on maize and sorghum in India is currently achieved using chemical insecticides. However, biological control using entomopathogens is a viable alternative tool for its long term sustainable management and at the same time preserving environment and human health. Infection of FAW larvae by different entomopathogens has been reported earlier in India[3–7].

The present study explored the natural occurrences of native entomopathogens on FAW from some of the intensive maize growing regions of Karnataka and Tamil Nadu in order to develop them into microbial biopesticides in future. Survey on the occurrence of these natural entomopathogens was undertaken on maize fields during the crop *kharif* season of 2019–20 at *Gauribidanur (*13.61°N, 77.51°E), Yaluvahalli (13.37°N, 77.71°E) and Mallur (13.34°N, 77.81°E) villages of Chikkaballapura district in Karnataka and Palacode (12.29°N, 78.07°E), Pappa-rapatti (12.20°N, 78.05°E), Kambainallur (12.20°N, 78.31°E) villages of Dharmapuri district; Udumalpettai (10.58°N, 77.25°E) of Thirupur district; Pollachi (10.66°N, 77.00°E) of Coimbatore district in Tamil Nadu. Thirty maize plants (forty days old) on a random from each field in each village were observed to document the natural occurrences of FAW and their entomopathogens. Single

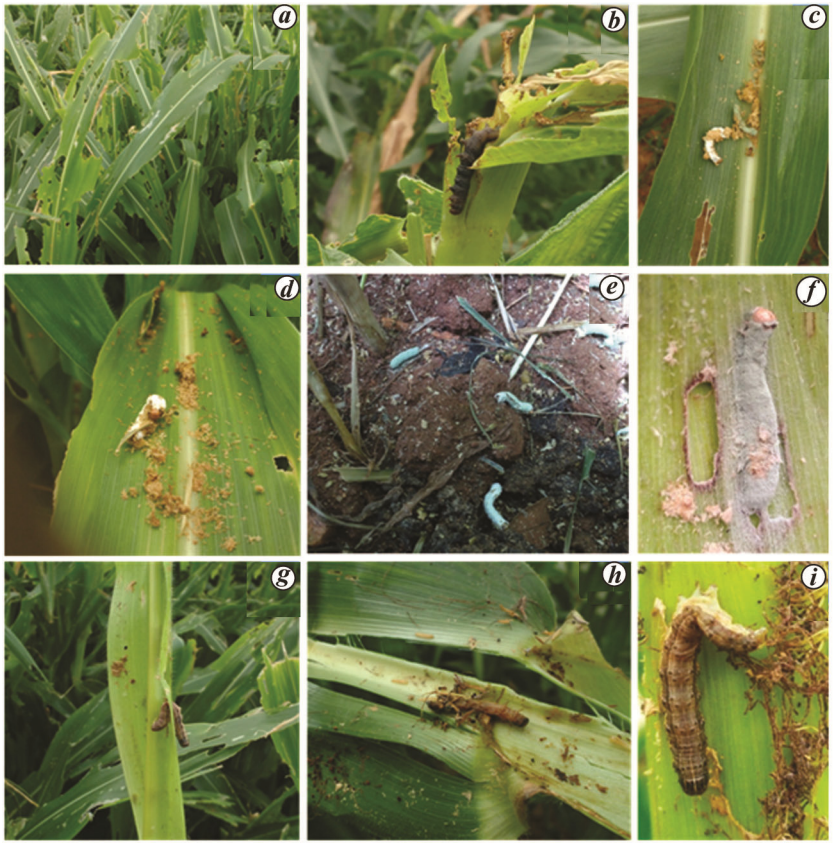

Figure 1. ***a***, Fall armyworm (FAW) infestation in maize. ***b***, Black coloured *Bacillus thuringiensis* infected FAW larvae. ***c–f***, *Nomuraea rileyi* infected FAW larvae (white and green coloured body covering). ***g–i***, NPV infected FAW larvae.